Block-Krylov Component Synthesis with Ritz Realization Algorithm for Structural Damage Detection

Fabio Guilherme Ferraz
José Maria C. Dos Santos

State University of Campinas
Dept. of Computational Mechanics
13083-970 Campinas S.P.
BRAZIL
fafe@fem.unicamp.br
zema@fem.unicamp.br

Abstract. *This paper explores the use of Block-Krylov Component Synthesis (BKCS) and Minimum Rank Perturbation Theory (MRPT) with Ritz Realization Algorithm (RRA) as a structural damage detection tool. BKCS is a simple and accurate method for generating a set of component Ritz vectors for use in component synthesis. Ritz vectors are obtained from derived recurrence relations, which represent a suitable basis vectors as an alternative to component normal vibration modes. MRPT is a model-based damage detection method, which utilizes the fact that discrete damage is manifested in a structural finite element model as a low rank perturbation to the structural property matrices. RRA convert the discrete time system matrices identified by Eigensystem Realization Algorithm (ERA) to continuous time system matrices, from which one can extract the experimental Ritz vectors used to complement the matrix of dynamic residual forces in the MRPT formulation. In this paper, the BKCS method is used in the fixed interface methodology along with an analytical finite element beam model subdivided in components. With the coupled healthy model and the measured damaged model, the MRPT with RRA is used to detect the damage location and his extent, or at least the component that contains the damage. Different substructure modeling assumptions on damage detectability are explored using numerical studies.*

Keywords:. *Ritz Vectors, ERA , Damage Detection ,Modal Synthesis, Complex Structures.*

1. Introduction

Some types of structural systems, such as, aircraft, spacecraft, bridges, and offshore platforms are exposed to damage in their service life. In order to assure safety, it is desirable that this structures be monitored to detect the damage occurrence, its location, and extent. The response to dynamic excitation of a complex structure is usually obtained by finite element model (FEM), which can be modeled with thousands of degree of freedom (DOF), and may have many components (substructures) that are often designed and produced by different organizations. Thus, model complexity demands for a substructure methodology to obtain a reduced system representation.

Component mode synthesis (CMS) is a substructuring method that consist in to modeling individual components of a structure separately, and couple them to form an assembled system. The CMS methods can be categorized according to the treatment of interface connection (Hurty, 1965). Each component is modeled by a set of vectors containing subsets of component normal modes augmented with other vectors, such as, constrained modes (Craig and Bampton, 1968) or attachment modes (Craig and Chang, 1977). However, the CMS can be generalized to permit the use of other shape vectors rather than normal modes. Developed by Craig and Hale, 1988, Block-Krylov Component Synthesis (BKCS) is a substructuring method which is based in this concept and was applied in this work with the fixed interface methodology. The method consist in to obtain a block-Krylov subspace through a simple recurrence relations, representing a suitable basis vector as an alternative to component normal modes. Repeated application of the recurrence relations generates a set of component vectors. The subspace spanned by the Ritz vectors is a block-Krylov subspace. Ritz vectors have been used extensively in the analytical and numerical areas of model reduction, eigensystem computation, transient response prediction, including CMS (Nour-Omid and Clough, 1984; Craig *at al*, 1988). The Ritz Realization Algorithm (RRA) was developed by Zimmerman, 1999, which have shown in his paper some advantages in use experimental Ritz vectors instead mode shapes along with Minimum Rank Perturbation Theory – MRPT (Zimmerman and Kaouk, 1994) to detect damage in structural systems. Motivated by the fact that Ritz vectors appear to be more sensitive to damage than traditional mode shapes, the RRA, is used in this work as an extension to MRPT.

The algorithm for damage detection is based on the original n DOFs, m_a block-Krylov component vectors obtained from the healthy structure, and m_e measured normal modes or Ritz vectors from the damaged structure. The block-Krylov component vectors of each substructure are used to form an assembled system model. With this model and the measured damaged normal modes or Ritz vectors, damage detection algorithm uses the MRPT with RRA technique to provide the indication of damage, his extent, or the component that contain the damage.

2. Block-Krylov Component Synthesis Method

The equation of motion of a typical undamped component α can be written as

$$\mathbf{M}\ddot{\mathbf{u}} + \mathbf{K}\mathbf{u} = \mathbf{f} \tag{1}$$

where **M** and **K** are the physical mass and stiffness matrices of the component, respectively, **u** is the displacement vector, and **f** is the force vector. We can also write the equation (1) in a partitioned form as

$$\begin{bmatrix} \mathbf{M}_{ii} & \mathbf{M}_{ij} \\ \mathbf{M}_{ji} & \mathbf{M}_{jj} \end{bmatrix} \begin{Bmatrix} \ddot{\mathbf{u}}_i \\ \ddot{\mathbf{u}}_j \end{Bmatrix} + \begin{bmatrix} \mathbf{K}_{ii} & \mathbf{K}_{ij} \\ \mathbf{K}_{ji} & \mathbf{K}_{jj} \end{bmatrix} \begin{Bmatrix} \mathbf{u}_i \\ \mathbf{u}_j \end{Bmatrix} = \begin{Bmatrix} \mathbf{f}_i \\ \mathbf{f}_j \end{Bmatrix} \tag{2}$$

where the subscripts i and j denotes partitions corresponding to N_i and N_j substructure DOFs at the interior and junction, respectively.

In component modal synthesis, the component displacement coordinates **u** are related to a reduced set of generalized coordinates **p** by the following Ritz transformation

$$\mathbf{u} = \mathbf{\Psi p} \tag{3}$$

where $\mathbf{\Psi}$ is a matrix whose columns are the component modes. Generally, the types of modes that make up $\mathbf{\Psi}$ are: constraint modes, attachment modes and normal modes.

The BKCS with the fixed interface uses the constraint modes, and the component normal modes are replaced by a set of Krylov vectors. A constraint mode is defined as the static deflection of a structure when a unit displacement is applied to one coordinate of a specific set of coordinates, while the remaining coordinates of that set are restrained and the remaining DOFs of the structure are force free. These constraint modes $\mathbf{\Psi}_c$ are obtained by solving the equation

$$\begin{bmatrix} \mathbf{K}_{ii} & \mathbf{K}_{ij} \\ \mathbf{K}_{ji} & \mathbf{K}_{jj} \end{bmatrix} \begin{Bmatrix} \mathbf{\Psi}_{ic} \\ \mathbf{I}_{cc} \end{Bmatrix} = \begin{Bmatrix} \mathbf{0}_{ic} \\ \mathbf{R}_{cc} \end{Bmatrix} \tag{4}$$

yielding

$$\mathbf{\Psi}_c = \begin{bmatrix} \mathbf{\Psi}_{ic} \\ \mathbf{I}_{cc} \end{bmatrix} = \begin{bmatrix} -\mathbf{K}_{ii}^{-1} & \mathbf{K}_{ij} \\ \mathbf{I}_{cc} & \end{bmatrix} \tag{5}$$

The BKCS is suggested by recurrence relations, which can be derived from the component dynamic equation

$$\left(\mathbf{K} - \omega^2 \mathbf{M}\right)\boldsymbol{\phi} = \mathbf{g} \tag{6}$$

where, ω^2 is an eigenvalue and $\boldsymbol{\phi}$ is the correspondent eigenvector of the component, and **g** constitutes boundary forces imposed on the component by adjacent components.

Let the equation (6) be written in partitioned form

$$\begin{bmatrix} \mathbf{K}_{ii} & \mathbf{K}_{ij} \\ \mathbf{K}_{ji} & \mathbf{K}_{jj} \end{bmatrix} \begin{Bmatrix} \boldsymbol{\phi}_i \\ \boldsymbol{\phi}_j \end{Bmatrix} = \omega^2 \begin{bmatrix} \mathbf{M}_{ii} & \mathbf{M}_{ij} \\ \mathbf{M}_{ji} & \mathbf{M}_{jj} \end{bmatrix} \begin{Bmatrix} \boldsymbol{\phi}_i \\ \boldsymbol{\phi}_j \end{Bmatrix} + \begin{Bmatrix} \mathbf{0} \\ \mathbf{g}_i \end{Bmatrix} \tag{7}$$

The top portion can be solved for $\boldsymbol{\phi}_i$ and the result combined with an identity for $\boldsymbol{\phi}_j$ to give

$$\boldsymbol{\phi} \equiv \begin{Bmatrix} \boldsymbol{\phi}_i \\ \boldsymbol{\phi}_j \end{Bmatrix} = \begin{bmatrix} -\mathbf{K}_{ii}^{-1}\mathbf{K}_{ij} \\ \mathbf{I} \end{bmatrix} \{\boldsymbol{\phi}_j\} + \omega^2 \begin{bmatrix} \mathbf{K}_{ii}^{-1}\mathbf{M}_{ii} & \mathbf{K}_{ii}^{-1}\mathbf{M}_{ij} \\ \mathbf{0} & \mathbf{0} \end{bmatrix} \begin{Bmatrix} \boldsymbol{\phi}_i \\ \boldsymbol{\phi}_j \end{Bmatrix} \tag{8}$$

or in abbreviated form the following *fixed interface recurrence formula* may be defined

$$\boldsymbol{\phi}^{(k)} = \mathbf{\Psi}_c \boldsymbol{\phi}_j^{(k)} + \omega^2 \mathbf{G}_c \boldsymbol{\phi}^{(k-1)} \qquad k = 1,2,\ldots \tag{9}$$

where *k* is the recurrence index, $\mathbf{\Psi}_c$ is the constraint mode matrix defined by Eq. (5), and $\mathbf{G}_c$ is defined by

$$\mathbf{G}_c = \begin{bmatrix} \mathbf{K}_{ii}^{-1}\mathbf{M}_{ii} & \mathbf{K}_{ii}^{-1}\mathbf{M}_{ij} \\ \mathbf{0} & \mathbf{0} \end{bmatrix} \tag{10}$$

Starting with $\boldsymbol{\phi}^{(0)} = 0$, apply equation (9) repeatedly to obtain

$$\boldsymbol{\phi}^{(k)} = \mathbf{\Psi}_c \boldsymbol{\phi}_j^{(k)} + \sum_{n=1}^{k-1} \omega^{2n} \mathbf{G}_c^{\,n} \mathbf{\Psi}_c \boldsymbol{\phi}^{(k-1)} \tag{11}$$

Equation (11) shows that $\boldsymbol{\phi}$ is a combination of the vectors in $\mathbf{\Psi}_c$, $\mathbf{\Psi}_c\mathbf{G}_c$, $\mathbf{\Psi}_c\mathbf{G}_c^{\,2}$, etc. Thus, a component fixed interface block-Krylov subspace will be defined by

$$\mathbf{\Psi}_c^k \equiv \left[\mathbf{\Psi}_c, \mathbf{\Psi}_c^{(1)}, \mathbf{\Psi}_c^{(2)}, \ldots, \mathbf{\Psi}_c^{(k-1)}\right] \tag{12}$$

where $\mathbf{\Psi}_c$ is given by equation (5), and where

$$\mathbf{\Psi}_c^{(r)} = \begin{bmatrix} \mathbf{\Psi}_{ic}^{(r)} \\ \mathbf{0} \end{bmatrix} = \mathbf{G}_c^{(r)} \mathbf{\Psi}_c \tag{13}$$

Then,

$$\mathbf{\Psi}_c^{(1)} = \begin{bmatrix} \mathbf{\Psi}_{ic}^{(1)} \\ \mathbf{0} \end{bmatrix} = \mathbf{G}_c \mathbf{\Psi}_c = \begin{bmatrix} \mathbf{K}_{ii}\left(\mathbf{M}_{ii}\mathbf{\Psi}_{ic} + \mathbf{M}_{ij}\right) \\ \mathbf{0} \end{bmatrix} \tag{14}$$

and subsequently,

$$\boldsymbol{\Psi}_c^{(r)} = \begin{bmatrix} \mathbf{K}_{ii}^{-1}\mathbf{M}_{ii}\boldsymbol{\Psi}_{ic}^{(r-1)} \\ \mathbf{0} \end{bmatrix} \qquad r = 2,3,\ldots,m_a \tag{15}$$

The deformation modes that characterize $\boldsymbol{\Psi}_c^{(r)}$ have fully restrained boundary DOFs, and the interior displacement is the static deflection due to inertia loading associated with the preceding deflection shapes of $\boldsymbol{\Psi}_c^{(r-1)}$. The vectors are orthogonalized at each step by the Gram-Schmidt orthogonalization and normalized with the mass matrix. A detailed development of this method can be found in Craig and Hale (1988). In this work, columns of $\boldsymbol{\Psi}_c^{(r)}$ are used to form a set of component vectors for the BKCS method. The Ritz coordinate transformation of Eq.(3) leads to the reduced-order undamped component model equation in generalized coordinates

$$\boldsymbol{\mu}\ddot{\mathbf{p}} + \boldsymbol{\kappa}\mathbf{p} = \boldsymbol{\Psi}^{\mathrm{T}}\mathbf{f} \tag{16}$$

where

$$\boldsymbol{\mu} = \boldsymbol{\Psi}^{\mathrm{T}}\mathbf{M}\boldsymbol{\Psi}, \qquad \boldsymbol{\kappa} = \boldsymbol{\Psi}^{\mathrm{T}}\mathbf{K}\boldsymbol{\Psi} \tag{17}$$

are the generalized mass and stiffness matrices respectively.

To illustrate the procedure for coupling components to form the reduced-order system model, consider two components, α e β, and let the generalized matrices be

$$\mathbf{p} = \begin{bmatrix} \mathbf{p}^{\alpha} \\ \mathbf{p}^{\beta} \end{bmatrix}, \qquad \boldsymbol{\mu} = \begin{bmatrix} \boldsymbol{\mu}^{\alpha} & \mathbf{0} \\ \mathbf{0} & \boldsymbol{\mu}^{\beta} \end{bmatrix}, \qquad \boldsymbol{\kappa} = \begin{bmatrix} \boldsymbol{\kappa}^{\alpha} & \mathbf{0} \\ \mathbf{0} & \boldsymbol{\kappa}^{\beta} \end{bmatrix} \tag{18}$$

Compatibility of interface displacement, and other linear equations constraints may be collected to form the constraint equation

$$\mathbf{C}\mathbf{p} = \mathbf{0} \tag{19}$$

Craig, 1981, indicate how the constraint matrix **C** can be used to define a coupling matrix **S**, that, in turn, defines a set of independent system coordinates **q**, i.e.,

$$\mathbf{p} = \mathbf{S}\mathbf{q} \tag{20}$$

Thus, the coupled system equations of motion is

$$\mathbf{M}_s\ddot{\mathbf{q}} + \mathbf{K}_s\mathbf{q} = \mathbf{0} \tag{21}$$

where

$$\mathbf{M}_s = \mathbf{S}^{\mathrm{T}}\boldsymbol{\mu}\mathbf{S}, \qquad \mathbf{K}_s = \mathbf{S}^{\mathrm{T}}\boldsymbol{\kappa}\mathbf{S} \tag{22}$$

If truncated sets of component vectors are used, matrices $\mathbf{M}_s$ and $\mathbf{K}_s$ will be find in reduced form, and a Ritz transformation back is necessary to return to the physical coordinates. The final mass and stiffness matrices so generated will be rank deficient, and this problem can be avoided using a complete set of component Ritz vectors which are easy and fast to be generated.

3. Minimum Rank Perturbation Theory and Subspace Selection Algorithm

A brief overview of MRPT for undamped structures is presented in which the mass matrix is assumed correct. A detailed development can be found in Zimmerman and Kaouk (1994). The goal is to determine a minimum rank perturbation matrix to the stiffness matrix such that the measured and analytical modal properties are in agreement. The eigenproblem for the structure with *p* measured eigenvalues can be written as

$$\left(\mathbf{K} - \omega_{di}^2\mathbf{M}\right)\boldsymbol{\phi}_{di} = \Delta\mathbf{K}_d\boldsymbol{\phi}_{di} \equiv \mathbf{b}_i \qquad i = 1,2,\ldots,p \tag{23}$$

The matrix $\Delta\mathbf{K}_d$ is the stiffness loss to be determined, $\boldsymbol{\phi}_{di}$ is the measured mode shape, ω_{Ii}^2 is the corresponding natural frequency, and $\mathbf{b}_{\mathrm{i}}$ is the dynamic residual vector. Equation (23) can be written in matrix form as

$$\mathbf{K}\boldsymbol{\Phi}_d - \mathbf{M}\boldsymbol{\Phi}_d\boldsymbol{\Lambda}_d = \Delta\mathbf{K}_d\boldsymbol{\Phi}_d \equiv \mathbf{B} \tag{24}$$

It should be noted that **B** can be calculated from equation (24) in terms of the measured modal properties and the original synthesized FEM matrices in physical coordinates. The matrix **B** is the dynamic modal residual matrix. By applying the MRPT concept in Eq. (24) $\Delta\mathbf{K}_d$ can be written as

$$\Delta\mathbf{K}_d = \mathbf{B}\left(\mathbf{B}^{\mathrm{T}}\boldsymbol{\Phi}_d\right)^{-1}\mathbf{B}^{\mathrm{T}} \tag{25}$$

Due to errors present in the measured modal data, a perfect zero/nonzero pattern of the dynamic residual $\mathbf{b}_i$ rarely occurs in practice. In this case the dynamic residual matrix **B** may lead to incorrect conclusions about the location of damage. To avoid this problem we can define $\mathbf{Z}_{di} = \mathbf{K} - \omega_{di}^2\mathbf{M}$ and write equation (23) as

$$\mathbf{b}_i^j \equiv \mathbf{z}_{di}^j\boldsymbol{\phi}_{di} = \left\|\mathbf{z}_{di}^j\right\|\left\|\boldsymbol{\phi}_{di}\right\|\cos\left(\theta_i^j\right) \tag{26}$$

where b_i^j is the *j*th DOF of the *i*th damage vector, $\mathbf{z}_{di}^j$ is the *j*th row of the matrix $\mathbf{Z}_{di}$ and θ_i^j is the angle between the vectors $\mathbf{z}_{di}^j$ and $\boldsymbol{\phi}_{di}$. A better indication of damage can be done through the deviation of the angle from ninety degrees,

$$\alpha_i^j = \theta_i^j\left(\frac{180^o}{\pi}\right) - 90^o \tag{27}$$

where θ_i^j is obtained from equation (26), α_i^j is the *j*th component of angle residual vector $\boldsymbol{\alpha}_i$, and the damaged DOFs are the components substantially different than zero degrees. In analogous form to matrix **B**, it is possible to assembly a matrix **A** (*angle residual matrix*) of the *p* measured eigenparameters, i.e.: $\mathbf{A} = [\boldsymbol{\alpha}_1, \boldsymbol{\alpha}_2, \boldsymbol{\alpha}_3, ..., \boldsymbol{\alpha}_p]$.

Consider the MRPT perturbation matrix constraint equation. The subspace selection algorithm (Zimmerman and Simmermacher, 1994) can be defined as a search for a matrix $\mathbf{X} \in R^{pxt}$ such that,

$$\Delta\mathbf{K}\boldsymbol{\Phi}_d\mathbf{X} = \mathbf{B}\mathbf{X} \tag{28}$$

is well conditioned. The unknowns are *t*, the numerical rank of **B**, and **X**. Consider the singular value decomposition (SVD) of **B**,

$$\mathbf{B} = \begin{bmatrix}\mathbf{U}_1 & \mathbf{U}_2\end{bmatrix}\begin{bmatrix}\boldsymbol{\Sigma} & \mathbf{0} \\ \mathbf{0} & \mathbf{0}\end{bmatrix}\begin{bmatrix}\mathbf{V}_1 & \mathbf{V}_2\end{bmatrix}^{\mathrm{T}} \tag{29}$$

where $\boldsymbol{\Sigma} \in R^{txt}$ is the matrix of non-zero (or grater than some prescribed tolerance) singular values, and **U** and **V** are the left and right singular vectors partitioned conformable. When **B** is rank deficient, its range is spanned by the *t* columns of $\mathbf{U}_1$. Thus, it is desired to find a **X** such that,

$$\mathbf{B}\mathbf{X} = \mathbf{U}_1 \tag{30}$$

The matrix **X** can be approximated by using the pseudo-inverse of **B** as

$$\mathbf{X} = \mathbf{B}^{+}\mathbf{U}_1 = \mathbf{V}_1\boldsymbol{\Sigma}^{+}\mathbf{U}_1^{\mathrm{T}}\mathbf{U}_1 = \mathbf{V}_1\boldsymbol{\Sigma}^{+} \tag{31}$$

Then, the stiffness loss, obtained by the solution of equation (28) is given by,

$$\Delta\mathbf{K} = \mathbf{B}\mathbf{X}\left(\mathbf{X}^{\mathrm{T}}\mathbf{B}^{\mathrm{T}}\boldsymbol{\Phi}_d\mathbf{X}\right)^{-1}\mathbf{X}^{\mathrm{T}}\mathbf{B}^{\mathrm{T}} \tag{32}$$

The columns of $\mathbf{U}_1$ represent the principle components of the dynamic residual matrix **B** or of the angle residual matrix **A**, which are termed ***principle component damage vectors***. An important improvement of this calculation is the noise reduction due to both measurements and substructure modeling errors.

4. Ritz Realization Algorithm

The RRA starts using the Engensystem Realization Algorithm - ERA (Juang and Pappa, 1985) to identify the discrete time system matrices **[A**, **B**, **C]**. The ERA, uses the impulse response of the structure gotten through an impulse response test, or by taking the inverse Discrete Fourier Transform (IDFT) of the frequency response functions measured from a broadband forced test of the structure. Thus, the generation of Ritz vectors start by converting the discrete time matrices to continuous time system matrices **[**$\mathbf{A}_c$, $\mathbf{B}_c$, **C]** using a method which assumes zero-order holds on the inputs. The first Ritz vector is obtained from the solution of

$$\mathbf{A}_c \mathbf{x}_1 = -\mathbf{B}_c \tag{33}$$

The static deflection $\mathbf{y}_1$ due to a unit load at the shaker location can be determined as

$$\mathbf{y}_1 = \mathbf{C}\mathbf{x}_1 \tag{34}$$

The subsequent vectors are generated from the recurrence relationship

$$\mathbf{A}_c \hat{\mathbf{x}}_i = \mathbf{x}_{i-1} \qquad i = 2,3,4,...,n \tag{35}$$

The vectors are orthogonalized at each step by the Gram-Schmidt orthogonalization procedure as

$$\mathbf{x}_i = \hat{\mathbf{x}}_i - \sum_{j=1}^{i-1} \mathbf{x}_j^{\mathrm{T}} \hat{\mathbf{x}}_i \mathbf{x}_j \tag{36}$$

After each vector is found, it is normalized to unit length, i.e., $\mathbf{x}_i^{\mathrm{T}} \mathbf{x}_i = 1$. The Ritz vector in the physical coordinates at the sensor location is computed as

$$\mathbf{y}_i = \mathbf{C}\mathbf{x}_i \tag{37}$$

All the vectors $\mathbf{y}_i$ are orthogonalized at each step by the Gram-Schmidt orthogonalization procedure and normalized with the mass matrix . The measured Ritz vectors can be represented as $\mathbf{V}_e = [\mathbf{y}_1, \mathbf{y}_2, \mathbf{y}_3, ..., \mathbf{y}_n]$.

5. Extension of MRPT for Experimental Ritz Vectors

Static Ritz Vectors

As stated above, the first computed Ritz vector is the structural static deflection due to a unit load at the shaker location. The static Ritz vectors can be represented as

$$\mathbf{K}[\hat{\mathbf{y}}_1 \cdots \hat{\mathbf{y}}_r] - [\mathbf{f}_1 \cdots \mathbf{f}_r] = \Delta\mathbf{K}_d \mathbf{V}_s \equiv \mathbf{B}_s \tag{38}$$

where $(\hat{\mathbf{y}}_i, \mathbf{f}_i)$ represent one of the r static deflection/load pairs. The matrix $\mathbf{B}_s$ represents the static Ritz residual matrix and, $\mathbf{V}_s = [\hat{\mathbf{y}}_1, \hat{\mathbf{y}}_2, \hat{\mathbf{y}}_3, ..., \hat{\mathbf{y}}_n]$. Thus, if the system matrices are obtained from test with only one input location and multiple output (SIMO), we can get only one static Ritz vector, i.e. $\mathbf{V}_s = \hat{\mathbf{y}}_1$. The minimum rank solution for $\Delta\mathbf{K}_d$ is given as,

$$\Delta\mathbf{K}_d = \mathbf{B}_s (\mathbf{B}_s^{\mathrm{T}} \mathbf{V}_s)^{-1} \mathbf{B}_s^{\mathrm{T}} \tag{39}$$

Dynamic Ritz Vectors

The dynamic Ritz vectors are defined as successive Ritz vectors with inertial correction which are computed starting with the static Ritz vector as $\mathbf{v}_1$, and applying successively the following equation

$$\hat{\mathbf{v}}_i = \mathbf{K}^{-1}\mathbf{M}\mathbf{v}_{i-1} \tag{40}$$

In this work, the orthogonalization and mass-normalization procedure at each step are done by the Lanczos Algorithm (Nour-Omid, 1984). The dynamic Ritz vectors so generated are used to replace $\boldsymbol{\phi}_{di}$ in Eq. (26) and to find the Ritz angle residual vectors $\boldsymbol{\alpha}_i$ that compose the Ritz angle residual matrix **A**. Subsequent application of the subspace selection in **A** produce the Ritz principle component damaged vectors $\mathbf{U}_1$. To avoid errors during the recurrence process of Eq. (40), the synthesized mass and stiffness matrices can not be rank deficient, i.e. it must not be adopted truncation of component sets of vectors in the BKCS method. Equation (40) can be written in matrix form as

$$\mathbf{M}\mathbf{V}_e + \mathbf{K}\mathbf{V}_d = \Delta\mathbf{K}\mathbf{V}_d \equiv \mathbf{B}_d \tag{41}$$

where, $\mathbf{V}_d = [\hat{\mathbf{v}}_1, \hat{\mathbf{v}}_2, \hat{\mathbf{v}}_3, ..., \hat{\mathbf{v}}_n]$, $\mathbf{V}_e$ is the matrix of measured Ritz vectors and $\mathbf{B}_d$ is the dynamic Ritz residual matrix. From Eq. (41), $\Delta\mathbf{K}_d$ can be determined as,

$$\Delta\mathbf{K}_d = \mathbf{B}_d (\mathbf{B}_d^{\mathrm{T}} \mathbf{V}_d)^{-1} \mathbf{B}_d^{\mathrm{T}} \tag{42}$$

6. Simulation Examples

Figure 1 shows the same structure used by Dos Santos and Zimmerman, 1996. It is a 2-dimensional clamped-clamped beam with 18 nodes, 3 DOFs/nodes and was artificially divided into 5 substructures.

To simulate the realistic case of noisy measurements, the eigenvectors were corrupted with a random noise of the form

$$\hat{\phi}_{ij} = \phi_{ij} + \phi_{ij}(\alpha/100) rand[-1,1] + rms(\phi_j)(\beta/100) rand[-1,1] \tag{43}$$

where, $\widehat{\phi}_{ij}$ is the noise corrupted shape vector element, ϕ_{ij} is the *i*th component of the *j*th shape vector, α and β are the scale and bias noise factors respectively, *rms*(ϕ_j) is the root mean square of the *j*th shape vector, and *rand*[-1,1] is a random number generator uniformly distributed between -1 and 1. It is assumed that only the first five modes of vibration are "measured".

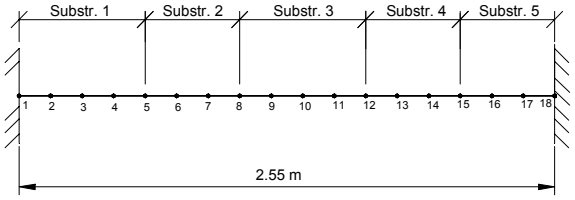

Figure 1 – Simulated example

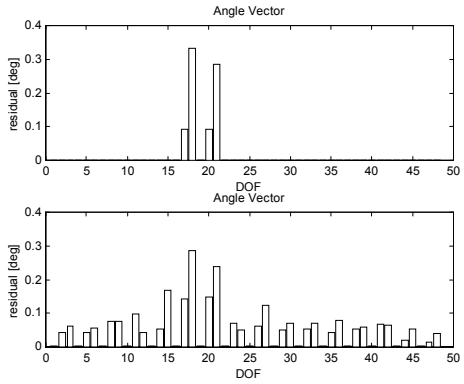

Figure 2 – Damage Localization without and with noise

Figure 2 shows the exact damage location (substructure S2, element 7, damaged DOFs 16-21) using angle residual approach without and with corrupted noise eigenvectors with 5% scale and 0.1% bias noise. The damage is characterized by 75% reduction in the original finite element inertia moment. It can be observed that the angle residual gives a strong indication to the location of damage in both cases.

Figure 3 shows three different sets of vector truncation (A, B and C) using modal angle residual vectors (MARV) and Ritz angle residual vectors (RARV) approaches. The damage is located in the element 1 (DOFs 1-6, substructure S1) with the same amount of damage imposed before. The three figures on the top use the MARV, and the other three on the bottom use the RARV. Five normal modes and dynamic Ritz vectors corrupted with 5% scale and 0.1% bias noise factors were used. The impulse response used in the ERA is obtained by taking the inverse fast Fourier transform of the frequency response functions measured from a simulated force test of the structure.

It can be observed that due to the component vectors truncation in sets A and B the MARV was able to find the location of damage, while the RARV was not. Using set C, which contains the complete base of component vectors, both were able to locate the damage. However, as it can be seen, the RARV seems to be less affected by measurement noise than the MARV.

Table 1 shows the quantity of vectors used in each set. The quantity of Ritz vectors in each block-Krylov corresponds to the number of DOFs in each component junctions, and the quantity of vectors used in these sets is obtained from columns of the block-Krylov vectors generated with the recurrence process of Eq. (15). By observing the graphics in Figure 3, one can see that most of them give an indication to the component that contains the damaged element. To quantify this indication, we use the ***component peak factor*** (CPF), which is defined as (Dos Santos and Zimmerman, 1996),

$$\mathbf{CPF} = \frac{1}{n_i}\left(\sum_{\substack{i=1 \\ j=1}}^{\substack{k \\ n_i}} \mathbf{U}_1(i,j) \right) \tag{44}$$

where $\mathbf{U}_1(i,j)$ is obtained through the $j = 1,2,...,k$ left singular vectors at the $i = 1,2,...,n_i$ substructure DOFs.

Figure 4 to Figure 6 show the extension of damage in the element 7 (DOFs 16 to 21) with damage level characterized by a 50% reduction in the original finite element inertia moment and using the vector set C. Figure 4 uses Eq. (32) with five normal modes corrupted with 5% scale and 0.1% bias noise factors. Figure 5 uses the same approach with five dynamic Ritz vectors instead of the normal modes, and the same noise factors was applied directly on the impulse response. And finally, the Figure 6 shows the exact damage extension. By observing these figures, it can be noted that the stiffness loss calculated with normal modes does not localize the damage, while the dynamic Ritz vectors provides a clear indication of location but the damage extension is still hard to quantify.

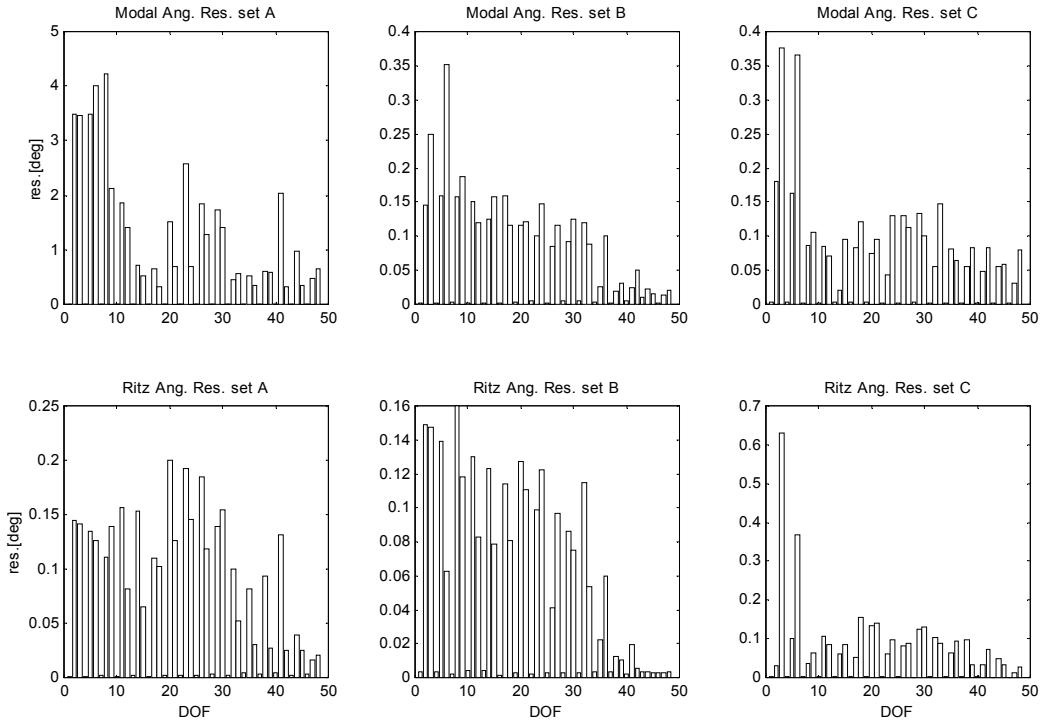

Figure 3 – MARV and RARV, Sets A to C with 5% scale and 0.1% bias noise factor

Table 2 contains the CPF results for each case in Figure 3, where it indicates substructure S1 in all the cases, as would be expected.

Table 1 – Component Vector Sets

Set	Substructure				
	S1	S2	S3	S4	S5
A	2	2	2	2	2
B	5	4	5	4	5
C	9	6	9	6	6

Table 2– Component Peak Factors

vector type	Set	Substructure				
		S1	S2	S3	S4	S5
Modal	A	0.48946	0.25498	0.19912	0.20332	0.14669
	B	0.39222	0.34280	0.26056	0.13898	0.05860
	C	0.38275	0.17923	0.29368	0.16545	0.10967
Ritz	A	0.42749	0.26335	0.31280	0.13122	0.07586
	B	0.39952	0.36212	0.34855	0.18517	0.04904
	C	0.34729	0.31486	0.26290	0.22431	0.12184

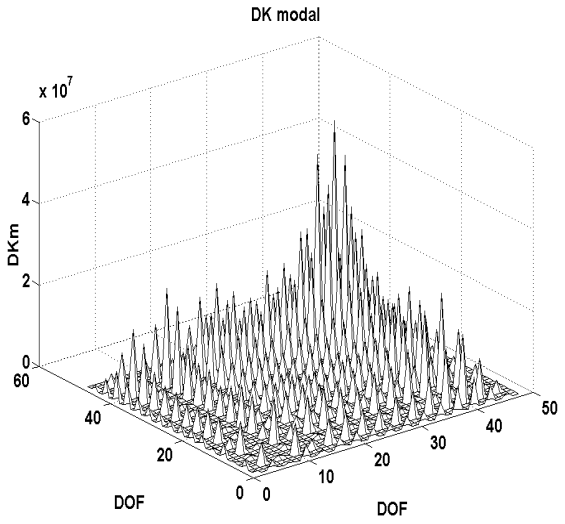

Figure 4 - Modal Result

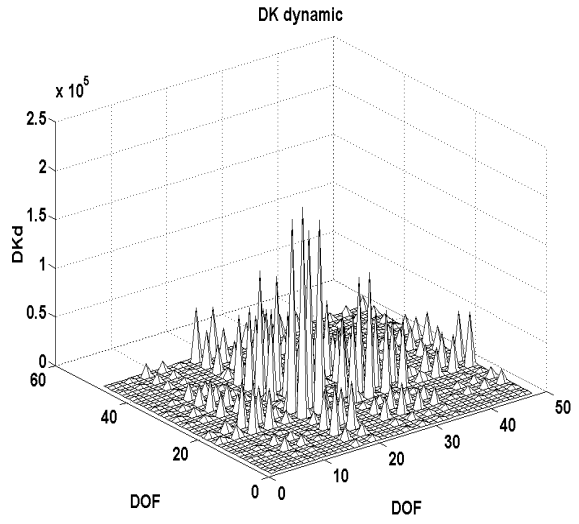

Figure 5 - Ritz Result

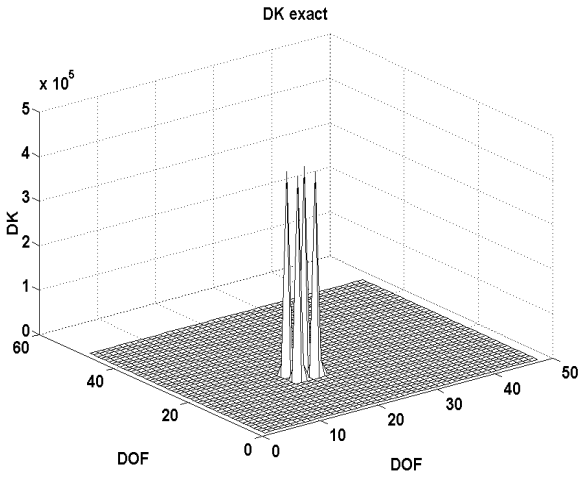

Figure 6 - Exact Result

The following figures (Figure 7 to Figure 14) show different cases of damage detection (damaged element 2, DOFs 1-6, substructure S1) using only the component vectors set C, with different noise factors, and different levels of damage imposed (characterized by reductions in the original finite element inertia moment). In these cases, the impulse response was generated without noise, and the simulated noise was applied directly on the normal modes and on the Ritz vectors. For each figure, 100 simulations runs were made. The difference in each run was the random noise generated in each measurement. These results show the mean and standard deviation of each component of the first and second principle component damage vectors of the angle residual vectors. The odd figures use the modal principle component damage vectors of the angle residual vectors (MPCV), and the pair figures use the Ritz vectors (RPCV). In the top of these graphs are indicated the DOFs that belong to the interfaces (+++) and the substructures. Table 3 summarizes the approaches used in each figure, and presents the CPF values obtained for each case.

It can be observed that in most of these simulations, the RPCV could locate the damage, even with high noise and low damage levels, and only in the last case, in Figure 14, with strongest noise factors (15% scale and 0.2% bias factors) and weakest damage imposed (25% reduction in the inertia moment) the RPCV was not able to locate the damage. However, the mode principle component vectors was able to indicate the damage location only in Figure 7, the one with the strongest level of damage, and in all other figures it could not locate the damage.

An interesting effect, observed by Dos Santos and Zimmerman, 1996, is that when the noise level is increased, (and when the damage level decreases) the importance of the second principle component vector becomes more important. That is because the perturbation of the vectors due to the noise is approaching the change in the vectors due to the damage. Thus, the magnitude, and therefore, the importance, of noise at each DOF is increased. This causes the first principle component to account for some of the noise. However, the second principle component is then able to more cleanly determine the location of the damage, or it works as a "filter" to the noise.

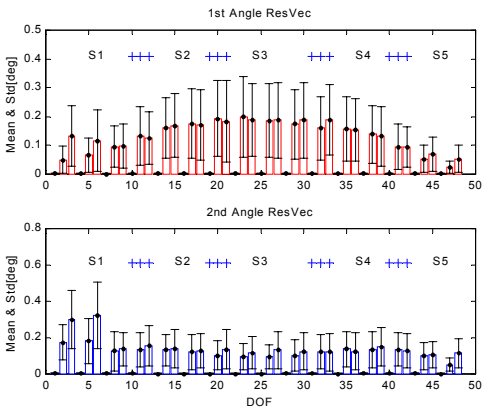

Figure 7 - MPCV. - noise [15 0.2] damage 75%

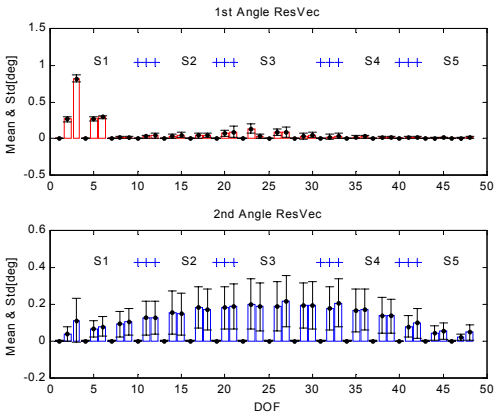

Figure 8 - RPCV - noise [15 0.2] damage 75%

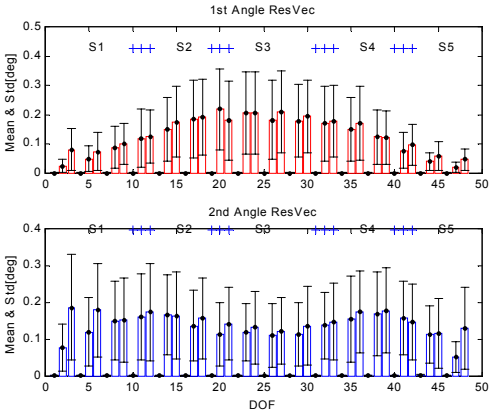

Figure 9 - MPCV - noise [10 0.1] damage 50%

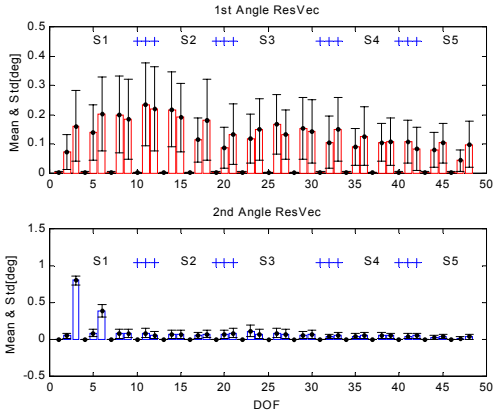

Figure 10 - RPCV - noise [10 0.1] damage 50%

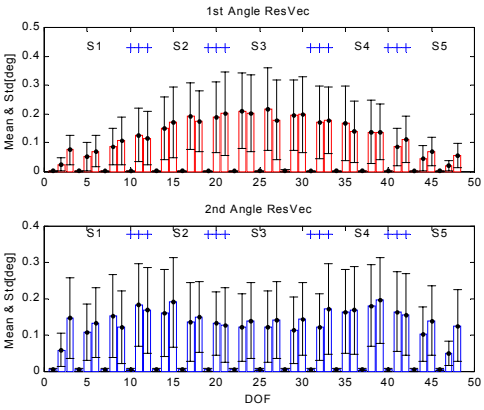

Figure 11 - MPCV - noise [5 0.1] damage 25%

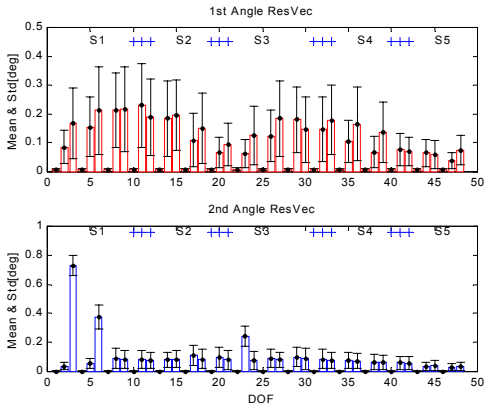

Figure 12 - RPCV - noise [5 0.1] damage 25%

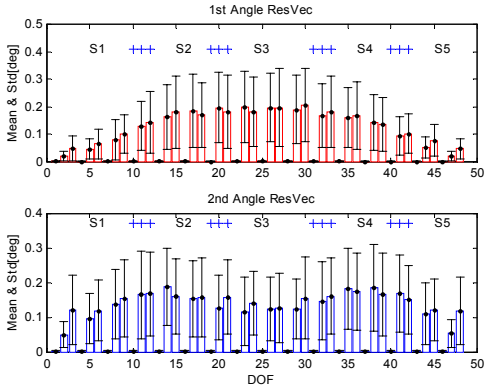

Figure 13 - MPCV - noise [15 0.2] damage 25%

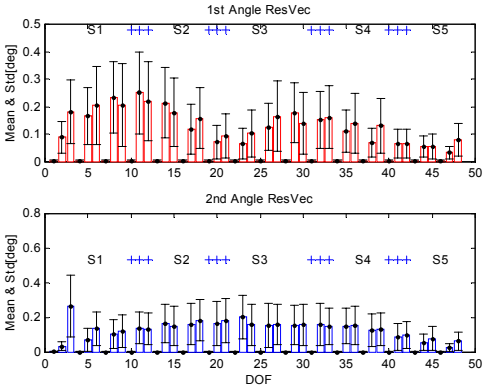

Figure 14 - RPCV - noise [15 0.2] damage 25%

Table 3 - Approaches and CPF results to Figure 7 to Figure 14

Fig.	Vector type	Noise	Damage: (red. in the inert. mom.)	CPF				
				S1	S2	S3	S4	S5
9	Normal modes	$\alpha = 15, \beta = 0.2$	75%	0.19728	0.19760	0.20113	0.18220	0.11515
10	Ritz vectors	$\alpha = 15, \beta = 0.2$	75%	0.20889	0.14109	0.17312	0.11336	0.04833
11	Normal modes	$\alpha = 10, \beta = 0.1$	50%	0.15712	0.21503	0.21494	0.19796	0.11956
12	Ritz vectors	$\alpha = 10, \beta = 0.1$	50%	0.25642	0.16405	0.13993	0.10907	0.08395
13	Normal modes	$\alpha = 5, \beta = 0.1$	25%	0.14741	0.21671	0.22138	0.20704	0.12776
14	Ritz vectors	$\alpha = 5, \beta = 0.1$	25%	0.25309	0.16324	0.15853	0.12793	0.07495
15	Normal modes	$\alpha = 15, \beta = 0.2$	25%	0.13974	0.22152	0.22128	0.20994	0.12656
16	Ritz vectors	$\alpha = 15, \beta = 0.2$	25%	0.21620	0.21898	0.19620	0.16645	0.08869

Conclusions

In this work an approach for structural damage detection using a substructure approach and residual force vector techniques is presented. The proposed procedure was verified using simulated measurements with modal parameters and experimental Ritz vectors obtained from a FEM of the assembled structure. The Ritz vectors extraction procedure involves the development of a state-space model of the system using measured time response. Ritz vectors can then be

extracted from this system realization. A correlated analytical FEM obtained with the BKCS method is used to locate damage regions by using MRPT with RRA techniques. The use of Ritz vectors instead of normal modes, results in some improvements to the damage detection algorithm:

Because Ritz vectors are generated from recurrence relations, his computational effort is less expensive then to compute eigenvectors and already includes the static correction term (Zimmerman, 1999).

In this study, the Ritz vectors used in the BKCS method is extracted directly from columns of block-Krylov vectors also generated from recurrence relations. Numerical examples suggest that only a few Ritz vectors should suffice to give good accuracy. Although synthesized matrices used in the RRA must be full rank, the Ritz vectors so generated have been shown more sensitive to damage than the corresponding modal parameters.

Must be recognized that this investigation represents only a limited test of this concepts. Further studies are currently underway to apply the method to a more realistic and complex substructured systems as well as experimental studies. The results presented indicate that the method is promising.

Acknowledgments

The authors are grateful to Fundação de Amparo a Pesquisa do Estado de São Paulo – FAPESP as well as the Conselho Nacional de Desenvolvimento Científico e Tecnológico – CNPq for the financial support given to this research.

References

Craig, R. R. Jr., 1981, “Structural Dynamics – An Introduction to Computer Methods”, Wiley, New York.

Craig, R. R. Jr., and Bampton, M. C. C., 1968, “Coupling of Substructures for Dynamic Analysis”, AIAA Journal, Vol. 7, pp. 1313-1319.

Craig, R. R. Jr., and Chang, C-J., 1977, “On the Use of Attachment Modes in Substructure Coupling for Dynamic Analysis”, Proceedings of the AIAA 19th Structures, Structural Dynamics, and Materials Conference, San Diego, CA, pp. 89-99.

Craig, R. R. Jr., and Hale, A. L., 1987, “Block-Krylov Component Synthesis Method for Structural Model Reduction”, Journal Guidance, Control, and Dynamics, Vol. 11, N. 6, pp. 562-570.

Craig, R. R. Jr., Kim, H. M., and Su, T. J., 1988, “Some Application of Lanczos Vectors in Structural Dynamics”, Proceedings of the 6th IMAC Conference, pp. 501-506.

Dos Santos, J.M.C. and Zimmerman, D.C., 1996, “Damage Detection in Complex Structures Using Component Mode Synthesis and Residual Modal Force Vector,” Proceedings of the 14th International Modal Analysis Conference, pp. 1299–1305.

Ferraz, F.G. and Dos Santos, J.M.C., 2001, "Block-Krylov Component Synthesis and Minimum Rank Perturbation Theory for Damage Detection in Complex Structures," Proceedings of the IX International Symposium on Dynamic Problems of Mechanics, pp. 329-334.

Hurty, W. C., 1965, “Dynamic Analysis of Structural Systems Using Component Modes, ”AIAA Journal, Vol. 3, pp. 678-685.

Juang, J.N. and Pappa, R. S. 1985 “An Eigensystem Realization Algorithm for Modal Parameter Identification,” J. Guidance and Control Dynamics, Vol.8, pp. 620-627.

Nour-Omid, B. and Clough, R. W., 1984, “Dynamic Analysis of Strucutres Using Lanczos Co-ordinates”, Earthquake Engineering and Structural Dynamics, Vol. 12, pp. 565-577.

Ojavo, I. U. and Pilon, D., 1988, “Diagnostics for Geometrically Locating Structural Math Model Errors From Modal Test Data”, Proceedings of the 29th AIAA/SDM Conference, Williamsburg, VA.

Wilson, E, L., Yuan, M.-Wu and Dickens, J. M., 1982, “Dynamic Analysis by Direct Superposition of Ritz Vectors”, ”, Earthquake Engineering and Structural Dynamics, Vol. 10, pp. 813-821.

Zimmerman, D. C., 1999, “Looking into the Crystal Ball: The Continued Need for Multiple Viewpoints in Damage Detection”, Key Engineering Materials, Vols. 167-168, pp. 76-90.

Zimmerman, D. C. and Kaouk, M., 1994, “Structural Damage Detection Usign a Minimun Rank Update Theory”, ASME Journal of Vibration and Acoustics, Vol. 116, pp. 222-231.

Zimmerman, D. C. and Simmermacher, 1994, “Model Refinement and System Health Monitoring Using Data from Multiple Static Loads and Vibration Test” Proceeding of the AIAA Dynamic Specialist Conference, SC.